

The contributions of surface charge and geometry to protein-solvent interaction

Soluble proteins are capacitors with net negative charge

Lincong Wang*

The College of Computer Science and Technology, Jilin University, Changchun, Jilin, China

To better understand protein-solvent interaction we have analyzed a variety of physical and geometrical properties of the solvent-excluded surfaces (SESSs) over a large set of soluble proteins with crystal structures. We discover that all have net negative surface charges and permanent electric dipoles. Moreover both SES area and surface charge as well as several physical and geometrical properties defined by them change with protein size via well-fitted power laws. The relevance to protein-solvent interaction of these physical and geometrical properties is supported by strong correlations between them and known hydrophobicity scales and by their large changes upon protein unfolding. The universal existence of negative surface charge and dipole, the characteristic surface geometry and power laws reveal fundamental but distinct roles of surface charge and SES in protein-solvent interaction and make it possible to describe solvation and hydrophobic effect using theories on anion solute in protic solvent. In particular the great significance of surface charge for protein-solvent interaction suggests that a change of perception may be needed since from solvation perspective folding into a native state is to optimize surface negative charge rather than to minimize the hydrophobic surface area.

1 Introduction

The quantification of protein-solvent interaction is essential for understanding protein folding, stability, solubility and function. Along with experimental studies considerable efforts have been made to quantify protein-solvent interaction using structures ever since the publication of the first protein crystal structure more than 50 years ago [1]. The solvent excluded surface (SES)¹ [2] of a protein is a two-dimensional (2D) manifold that demarcates a boundary between the protein and its solvent. An SES consists of three different types of area: solvent accessible area (SAA, a_s), torus accessible area (TAA, a_t) and probe accessible area (PAA, a_p). Geometrically a_s is a convex area, a_p a concave one and a_t a saddle area. Either SES or more frequently accessible solvent surface [3, 4] has been studied extensively for its role in protein-solvent interaction [5, 6, 4, 7, 8, 9, 10] since they could be computed readily using atomic coordinates and radii. Though much progress has been made in the past [11, 12] there is still a lack of accurate and robust algorithm and/or efficient implementation for SES computation and previous SES applications to protein-solvent interaction have been limited in several respects. Two most popular programs, PQMS [11] and MSMS [12], are neither robust nor accurate enough for a large-scale application. For example, both may require modification to atomic radii to handle singular cases of intersecting PAAs and tend to fail on large proteins with $>10,000$ atoms. A manual restart is needed for MSMS to compute each internal cavity inside a protein. The arbitrary modification to radii and manual restart introduce inconsistency and make them less suitable for accurate SES computation on a large scale. To overcome these difficulties we have developed a robust SES algorithm that treats all the possible probe intersecting cases

*Corresponding author: Lincong Wang, Email: wlincong@hotmail.com.

¹Abbreviations used: SES, solvent excluded surface; SEA, solvent excluded area; SA, solvent accessible; ASA, accessible solvent surface area; SAA, solvent accessible area (a_s); PAA, probe accessible area (a_p); TAA, torus accessible area (a_t); VDW, van der Waals; 2D, two-dimensional; 3D, three-dimensional; MD, molecular simulation; BSP, binary space partition; SSE, Streaming SIMD Extensions.

without any modification to atomic radius. It computes the internal cavity automatically with no manual intervention and achieves a high precision with an estimated error $< 3.0 \times 10^{-3} \text{Å}^2$ per surface atom for all the three types of SES areas². In our implementation any atom with $a_s > 3.0 \times 10^{-4} \text{Å}^2$ is defined as a surface atom. Previous SES applications to protein-solvent interaction have focused more on (1) accessible solvent surface area (ASA) [13, 9, 14, 10] rather than solvent-excluded surface area (SEA) likely due to the easy computation of the former, (2) individual residues rather than individual atoms and (3) surface area only rather than the geometrical and physical properties of the surface. A few studies [15, 16] have used atomic ASAs for example to predict solvent accessibility of amino acid residues. To our knowledge no atomic SES applications have been published up to now. The accuracy and robustness of our algorithm enable us to perform a statistical analysis on SES’s contribution to protein-solvent interaction over a set \mathbb{N} of 24, 024 soluble proteins with crystal structures by focusing on their individual atoms and using not only SEA but also SES’s geometrical and physical properties especially electrical properties. We discover that not only every structure in \mathbb{N} has a net negative surface charge and permanent electric dipole but the changes with protein size of surface charge, dipole and surface geometry as well as several physical and geometrical properties defined by them also follow well-fitted power laws³. For example, the charge per atom for all the surface atoms has an average of -29.6×10^{-3} coulomb over all the structures in \mathbb{N} while the charge per atom for all the atoms has an average of only -1.6×10^{-3} coulomb. Thus soluble proteins behave like an electric dipole or more properly a capacitor in solution. Moreover our analysis shows that on average the SEAs for hydrophilic atoms which are capable of forming a hydrogen bond with a solvent molecule are almost 2-fold larger than those for hydrophobic atoms. The larger the SEA of a surface atom is the better of its hydrogen bonding interaction with solvent. Geometrically we find that concave-convex ratio $r_{cc} = \frac{a_p}{a_s}$ increases with protein size and upon folding. The larger of r_{cc} of a surface atom is the flatter of its local surface. Most interestingly hydrophobic atoms have larger r_{cc} s than hydrophilic ones. One plausible explanation is that for a surface atom the larger its r_{cc} the better of its van der Waals (VDW) interaction with the solvent []. The relevance of these physical and geometrical properties to protein-solvent interaction is collaborated by the strong correlations between their values computed for individual amino acid residues and five well-known hydrophobicity scales [17, 18, 19, 20] and by their large changes upon protein unfolding. For example, the fitted solvation parameters (σ_i s) [7, 8] in solvation free energy-surface area relation, $\Delta G_{\text{solv}} = \sum_i \sigma_i \text{ASA}_i$ where ASA_i is the ASA for residue i , could be interpreted as surface charges. Previously no physical meanings have been given to these σ_i s. In addition our large-scale analyses of protein-ligand interfaces [21] where the ligand is either a DNA or a small-molecule compound or another protein show that (1) the values for these properties over the set of surface atoms that are buried upon ligand-binding differ largely from those over the set of atoms that remain exposed, and (2) ligand binding share many similarities with protein folding in terms of SES’s physical and geometrical properties.

How a protein interacts with solvent is of paramount importance for understanding protein folding. For example, it is widely accepted that hydrophobic effect is the driving force for protein folding [22, 23]. However, the nature of hydrophobic effect and the details of protein hydration shells remain unclear at present [24]. The findings presented here reveal fundamental but distinct roles of surface charge, hydrogen bonding and SES geometry for protein-solvent interaction and are consistent with water being a protic solvent that prefers anions over cations as its solutes. They shed new lights on hydrophobic effect by demonstrating that it is an effect to which both surface area and charge contribute and suggest that the optimization of protein solvation through natural selection is achieved by (1) universal enrichment of surface negative charge, (2) increased surface areas for hydrophilic atoms for better hydrogen bonding with solvent, and (3) higher concave-convex ratio for hydrophobic atoms for better VDW attraction with solvent. It seems to us that a paradigm shift may be required in the study of the protein-folding problem by focusing on surface charge rather than side chain hydrophobicity since folding into a native state is to maximize the negative surface charge rather than to minimize the hydrophobic surface area. The statistical values for the surface charge and dipole moment and the fitted power laws obtained on the large set of structures should be useful for the quantification of solvation and hydrophobic effect using well-known theories on anion solutes in protic solvent [25, 26, 27, 28, 29]. Furthermore the statistical values for SES-defined physical and geometrical properties could also be used to restraint the folding space for a protein or serve as a term in an empirical scoring function for protein structure prediction [30] or a quantity for quality control in structure determination [31]. *The relative importance of surface dipole, hydrogen-bonding and VDW attraction for protein-solvent interaction.*

²The total error E_r for a protein increases slowly with the number of atoms N : $E_r \propto \sqrt{N}$

³In this paper a linear equation $y = ax + c$ is treated as a special power law: $y = ax^b + c$ with $b = 1$.

2 Materials and Methods

In this section we first describe the data sets used in our statistical analysis and then briefly present our algorithm for SES computation. Finally we define a variety of SES-defined physical and geometrical properties for a protein that are relevant to its interaction with solvent.

2.1 The protein data sets

We have downloaded from the current version of the PDB a non-redundant set \mathbb{N} of 24,024 crystal structures each has >800 atoms (with protons) for a monomeric or >1000 atoms for a multimer, at most 70% sequence identity with any others, a resolution $\leq 3.5\text{\AA}$ and an R -factor $\leq 27.5\%$. The set \mathbb{N} excludes hyperthermophilic, membrane and nucleic acid binding proteins and the size (number of atoms n) of its structures ranges from 833 to 171,552 atoms. It is further divided into a set of monomers \mathbb{M} with 8,974 structures with sizes from 833 to 44,200 atoms and a set of multimers \mathbb{D} with 15,050 structures. Out of \mathbb{M} we select a subset \mathbb{M}_f of 1,766 monomeric structures that have no gap in sequence, no compounds with >5 atoms and $<0.2\%$ missing atoms. The set \mathbb{M}_f is used to represent soluble proteins in free state and whose structures have 1,004 to 10,297 atoms. Via the sequence information in \mathbb{M}_f a set of extended and energy-minimized conformations \mathbb{M}_u are generated using CNS [32] to study the changes in SES's physical and geometrical properties upon protein unfolding. Protons are added using the program REDUCE [33] to any PDB that lacks their coordinates. Please see the supplementary materials for the preprocessing of PDBs for SES computation.

2.2 The computation of solvent excluded surface

Solvent excluded surface (SES) is composed of three types of areas: solvent accessible area $a_s(i)$, torus accessible area $a_t(i, j)$ and probe accessible area $a_p(i, j, k)$ where $a_s(i)$ is a patch on the spherical surface of a single protein atom i , $a_t(i, j)$ a toric patch defined by two atoms i, j and $a_p(i, j, k)$ a patch on the surface of a probe whose position is determined by three atoms i, j, k . Geometrically a_s is a convex area, a_p a concave one and a_t a saddle area. Here we describe briefly the key steps of our algorithm. It starts with the determination of all the solvent accessible atoms \mathbb{S} on both the exterior and interior surfaces of a protein. For each pair of atoms in \mathbb{S} and any third protein atom, we compute the probe defined by the triple. Given the set of the computed probes \mathbb{P} , we exhaustively search for the intersections between any pair of probes. If there exists an intersection, the intersected area is removed from further considerations. Given set \mathbb{P} if any two probes share a pair of atoms, we compute the torus defined by the two probes and the two atoms. A subset of non-intersecting probes is selected if there exist overlappings among them. Both a_s and a_p are computed by counting the number of exposed vertices on a spherical surface that is represented by a set of uniformly-distributed 40,962 vertices while a_t is computed analytically. The algorithm is implemented in C++ with pthread for parallel computation, SSE for vector computation and Qt/openGL/GLSL for structure and surface visualization. Please see the supplementary materials (Fig. S1) for a comparison of the surfaces by MSMS and our program.

In this study we set the probe radius to 1.4\AA except for set \mathbb{M} over which SESs are computed twice using respectively 1.4\AA and 1.2\AA . The SESs with 1.2\AA radius are compared with those with 1.4\AA to see how the probe radius affects SES's physical and geometrical properties. The atomic radii used are: C = 1.70\AA , N = 1.55\AA , O = 1.52\AA , S = 1.75\AA , H = 1.09\AA and Se = 1.80\AA ;

2.3 The physical and geometrical properties of SES

A variety of physical and geometrical properties defined on SES have been computed to quantify their possible contributions to protein-solvent interaction. Those we find to be relevant are listed here and are called SES-defined properties for later reference. Their definitions rely on the assignment of charge and area to individual atoms.

2.3.1 The physical properties of SES

To each individual surface atom i we assign an atomic SEA $a(i)$.

$$a(i) = a_s(i) + a_t(i) + a_p(i); \quad a_t(i) = \frac{\sum_j a_t(i, j)}{2}, \quad a_p(i) = \frac{\sum_{j, k} a_p(i, j, k)}{3}. \quad (1)$$

where $a_s(i)$, $a_t(i)$ and $a_p(i)$ are respectively the solvent accessible, toric and probe areas for atom i . For a protein we define its SEA A , net surface charge Q_s and average-partial charge of the exposed atoms⁴ ρ_s .

$$A = \sum_i a(i), \quad Q_s = \sum_i e(i), \quad i \in \mathbb{S}$$

$$n_s = |\mathbb{S}|, \quad \rho_s = \frac{Q_s}{n_s} \quad (2)$$

where \mathbb{S} is the set of surface atoms with n_s atoms, $e(i)$ the partial charge of atom i whose value is taken from Charmm force field [10]. The area-weighted surface charge q_s and area-weighted surface charge density σ_s are defined as follows.

$$q_s = \sum_i a(i)e(i), \quad \sigma_s = \frac{q_s}{A}; \quad (3)$$

Set \mathbb{S} could be further divided into two subsets: $\mathbb{S} = \mathbb{S}^+ \cup \mathbb{S}^-$ where \mathbb{S}^+ and \mathbb{S}^- are respectively the sets of atoms with $e(i) \geq 0$ and $e(i) < 0$. For both subsets we define their respective average-atomic areas η_s^+ and η_s^- , area-weighted positive and negative surface charges q_s^+ and q_s^- , and area-weighted surface charge densities σ_s^+ and σ_s^- .

$$A^+ = \sum_i a(i), \quad n_s^+ = |\mathbb{S}^+|, \quad \eta_s^+ = \frac{A^+}{n_s^+}, \quad e(i) \geq 0$$

$$q_s^+ = \sum_i a(i)e(i), \quad \sigma_s^+ = \frac{q_s^+}{A^+}, \quad e(i) \geq 0$$

$$A^- = \sum_i a(i), \quad n_s^- = |\mathbb{S}^-|, \quad \eta_s^- = \frac{A^-}{n_s^-}, \quad e(i) < 0$$

$$q_s^- = \sum_i a(i)e(i), \quad \sigma_s^- = \frac{q_s^-}{A^-}, \quad e(i) < 0 \quad (4)$$

where n_s^+ and n_s^- are respectively the number of atoms in \mathbb{S}^+ and \mathbb{S}^- . For the set of buried atoms \mathbb{B} in a protein we define its net charge Q_b and average-partial charge ρ_b .

$$Q_b = \sum_j e(j), \quad j \in \mathbb{B}$$

$$n_b = |\mathbb{B}|, \quad \rho_b = \frac{Q_b}{n_b} \quad (5)$$

where n_b is the number of atoms in \mathbb{B} . Please note that the set of all the atoms for a protein $\mathbb{A} = \mathbb{B} \cup \mathbb{S}$. The net charge Q , average-partial charge ρ and charge Q_d of an electric dipole moment (or polarization vector) \vec{P} ⁵ for a protein (dipole charge in short) are defined as follows.

$$n = n_b + n_s, \quad Q = Q_b + Q_s, \quad \rho = \frac{Q}{n}$$

$$Q_d = Q_s - \frac{Q}{2} \quad (6)$$

where $n = |\mathbb{A}|$ is the total number of atoms.

⁴Solvent accessible, exposed and surface atoms are used interchangeably in this paper.

⁵ $\sigma_{pol} = \frac{Q_d}{V} = \vec{P} \cdot \mathbf{n}$ where V is the volume of the region enclosed by an SES, σ_{pol} the charge density and \mathbf{n} the surface normal.

To evaluate the contribution of the hydrogen bonds between a protein and its solvent to their interaction we divide \mathbb{S} into two subsets, \mathbb{S}_o of hydrophobic atoms and \mathbb{S}_i of hydrophilic atoms, with their respective surface areas A_o and A_i defined as follows.

$$\begin{aligned}\mathbb{S} &= \mathbb{S}_o \cup \mathbb{S}_i \\ A_o &= \sum_i a(i), \quad i \in \mathbb{O}; \quad n_o = |\mathbb{S}_o|, \quad \eta_o = \frac{A_o}{n_o} \\ A_i &= \sum_j a(j), \quad j \in \mathbb{I}; \quad n_i = |\mathbb{S}_i|, \quad \eta_i = \frac{A_i}{n_i}\end{aligned}\quad (7)$$

where n_o and n_i are their numbers of atoms, and η_o and η_i their average-atomic areas. The protein atoms in \mathbb{S}_i are either hydrogen bond donors or acceptors (H-bond capable in short⁶) while \mathbb{S}_o include the rest of atoms (see the supplementary materials for their definitions). The area A_i is called the polar surface area of a protein in short.

2.3.2 The geometry of SES

The SEA $a(i)$ for atom i is composed of three types of area: $a_s(i)$, $a_t(i)$ and $a_p(i)$ with $a_s(i)$ a convex area defined by a single atom i while $a_p(i)$ a concave area defined by three atoms i, j, k . For a set of surface atoms \mathbb{T} we define a convex-concave ratio r_{cc} to estimate their overall surface flatness and a sphere-volume over surface-volume r_{pp} to measure how tight a protein is packed.

$$\begin{aligned}r_{cc} &= \frac{\sum_i a_p(i)}{\sum_i a_s(i)}, \quad i \in \mathbb{T} \\ V_s &= \frac{4\pi}{3} \left(\frac{A}{4\pi}\right)^{3/2}, \quad V_a = \frac{4\pi}{3} \sum_k r_k^3, \quad k \in \mathbb{A} \\ r_{pp} &= \frac{V_s}{V_a}\end{aligned}\quad (8)$$

where A is the total SEA, V_s the surface-volume defined as the volume of a sphere with the same surface area as A , and V_a the sum of atomic volumes over \mathbb{A} and r_k the radius of atom k . Since the concave area a_p of a surface atom is determined by triples of protein atoms, we could use r_{cc} to estimate the contribution to protein-solvent interaction of VDW attraction.

3 Results and Discussion

In this section we present the SES-defined physical and geometrical properties over sets \mathbb{N} , \mathbb{M}_f and \mathbb{M}_u and discuss their significance for protein-solvent interaction.

3.1 Surface charge and electric dipole and polar surface area

Though it is well-documented that hydrophilic residues especially the charged ones prefer to be on a protein surface, surface charge is thought to be important for protein solubility⁷ and most important physical and chemical properties of a protein are ultimately related to the electrostatic interactions among its composing atoms and with other molecules such as solvent [34, 28], to our knowledge no large-scale surveys of surface charges have been reported. With atomic SEA and the separation of surface atoms from buried ones and the division of atoms into different subsets according to their physical-chemical properties (Eqs. 1–7), it is possible to evaluate the contributions of surface area and charge to protein-solvent interaction by performing a statistical analysis over known structures on physical and geometrical properties defined by them. In theory, evolution must have optimized soluble proteins for best interacting with water and since the latter is a protic solvent that prefers anions over cations we expect that folding into a

⁶In the rest of paper we use *H-bond capable atoms* and *hydrophilic atoms* interchangeably.

⁷R. P. Feynman tried to explain the protein salt-out effect by assuming the existence of negative charges on protein surfaces. “The molecule (protein) has various charges on it, and it sometimes happens that there is a net charge, say negative, which is distributed along the chain”, The Feynman Lectures on Physics, page 7–10, Vol.2.

Structures	Exposed (ρ_s)	Buried (ρ_b)	Total (ρ)	Exposed ($\rho_{\text{adj},s}$)	Buried ($\rho_{\text{adj},b}$)
\mathbb{M}_f	-26.6, 6.1	27.6, 7.9	-1.3, 2.4	-25.3, 4.7	28.9, 8.3
\mathbb{M}_u	0.7402, 2.9	-13.8, 33.4	0.2508, 2.5	0.4894, 1.2	-14.1, 33.7

Table 1: **The average-partial charges over the sets of exposed (S), buried (B) and total atoms (A) for the folded (\mathbb{M}_f) and unfolded (\mathbb{M}_u) structures.** The two numbers in each cell are respectively mean and standard deviation. The unit is $10^{-3} \times$ coulomb per atom. Some structures in \mathbb{M}_f may have no coordinates for the free amine groups at their N-termini and that leads to a negative mean for the ρ_s for the folded structures. The adjusted average-partial charges $\rho_{\text{adj},s}$ and $\rho_{\text{adj},b}$ are computed using the adjusted surface charge $Q_d = Q_s - \frac{Q}{2}$ for the folded and unfolded structures.

native state will turn a soluble protein into an anion with positive charges buried inside. Indeed we find that all the 24, 024 structures in \mathbb{N} have negative net surface charges (negative Q_s, q_s and ρ_s) and positive net buried charges (positive Q_b and ρ_b)⁸ (Fig. 1a) and more strikingly the difference in mean between average-partial charges ρ_e and ρ is more than 17-fold. It is equivalent to a 17-fold increase in negativity on average when a protein folds into a native state. In addition the net surface charges for the structures in \mathbb{M} remain to be negative even when the probe radius is reduced from 1.4Å to 1.2Å (see supplementary materials). More hydrophobic atoms become exposed with a smaller probe radius. Furthermore negative surface charges increase with protein size⁹ via well-fitted power laws and their enrichment is apparent upon folding. As shown in Table 1, the difference in ρ_s s between the folded structures (\mathbb{M}_f) and unfolded ones (\mathbb{M}_u) is >30 -fold on average. The extended conformations in \mathbb{M}_u may deviate from the real unfolded states existent in a typical experimental setting and thus the geometrical and electrical properties computed on them may have errors. However the large difference in ρ_s between \mathbb{M}_f and \mathbb{M}_u supports the relevance of surface charge to protein-solvent interaction. The findings described above together show that surface charge is a universal property importance for protein-solvent interaction.

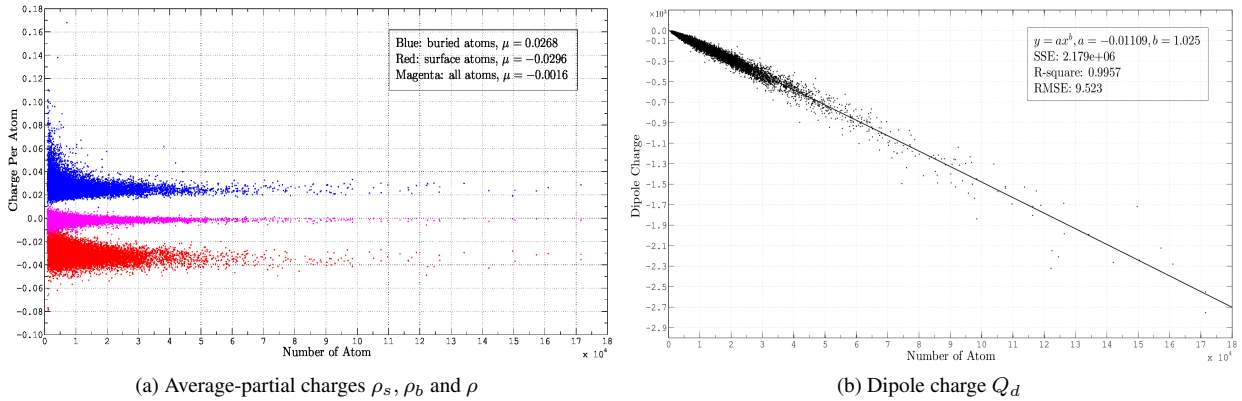


Figure 1: **Average-partial charges ρ_s, ρ_b, ρ and dipole charge Q_d .** (a) The average-partial charges ρ_s (colored in red), ρ_b (blue) and ρ (magenta) over \mathbb{N} . The mean value μ_s for ρ_b, ρ, ρ_s are respectively 0.0268, -0.0016 and -0.0296 , and the difference between the μ_s for ρ_s and ρ is >17 -fold. The y-axis is average-atomic charge in coulomb per atom. (b) Dipole charge Q_d s over \mathbb{N} . The change of Q_d s with protein size (n) could be fitted very well either to a power law $Q_d = an^b$ with a $R_{\text{square}} = 0.9957$ and $b = 1.025$ or a linear equation (data not shown). The y-axis is dipole charge in coulomb. The x-axes in both (a, b) are n , the total number of atoms in each structure.

All the structures in \mathbb{N} have small nonzero net charges (Q_s) with an average of $\rho = -0.0016$ coulomb per atom (Fig. 1a). The small negative ρ_s are due in part to the lack of coordinates for the free amine groups at protein's N-termini. To make a structure neutral in charge we define an adjusted surface charge $Q_d = Q_s - \frac{Q}{2}$. It is the

⁸Using the criteria listed in section 2.1 two structures (PDBIDs:3odv and 4uj0) have positive surface charges. Both of them are membrane-permeable toxins composed of several peptides. Another membrane-permeable small monomeric protein (PDBID:1bhp) with 658 atoms including protons also has positive surface charge. One structure (PDBID:1w3m, an antibiotic named tsumimycin) has very small net negative buried charge, $Q_b = -1.68$ coulomb. They are excluded in the present study for easy exposition.

⁹In this paper protein size could mean either n or n_s or A since they are related to each other via simple relationships (supplementary materials).

Structures	η_i	η_o	$\frac{A_o}{A_i}$	η^+	η^-	$\frac{A^+}{A^-}$
\mathbb{M}_f	19.1792	12.3654	1.2102	12.9688	17.061	1.1918
\mathbb{M}_u	16.1297	8.5199	1.5714	9.3988	13.2806	1.4865

Table 2: **The average-atomic areas of the folded (\mathbb{M}_f) vs unfolded (\mathbb{M}_u) structures.** In addition to the average-atomic areas the ratios $\frac{A_o}{A_i}$ and $\frac{A^+}{A^-}$ are listed respectively in the third and last columns. The unit for average-atomic areas is \AA^2 per atom.

charge for a permanent electric dipole moment \vec{P} . As shown in Fig. 1b, Q_d decreases almost linearly with protein size n , and most interestingly \vec{P} changes its direction upon protein folding (Table 1), that is, the signs of the surface charges Q_{s^+} and Q_{s^-} of the unfolded conformations change from being positive to negative upon folding. Thus \vec{P} is likely to be a universal quantity important for protein-solvent interaction. Taken together, it is clear that folding into a native state in solution turns a protein into a capacitor with a net negative charge on its SES, the outer surface of a capacitor, to maximize its attraction to the solvent [35]. Except for the charged side chain atoms Charrm partial charges [10] for a residue have zero net charge for its subgroups of bonded atoms and thus except for the regions where the charged side chain atoms are located, there must exist a 2D manifold (the inner surface of the capacitor) inside a soluble protein that encloses a set of atoms with zero net charge. A model of alternative layers of negative and positive charges has been alluded previously in molecular dynamic (MD) simulation [36]. Though the details of such a multi-layer model could not be worked out without knowing the 2D manifold for each layer, if proved to be correct it may provide an explanation to why the protein interior is like a medium of high polarizability.

The strength of the interaction between a polar solute and a protic solvent such as water is determined also by the hydrogen bonds between them while the strength of the latter depends on both distance and direction. Thus the larger the SEA of a hydrophilic atom has the stronger of its interaction with water since a larger SEA is less disruptive to water structure and thus causes less loss of solvent entropy. In theory the optimization via evolution must have maximized such polar surface areas. Indeed as shown in Fig. 2a the average-atomic areas (η_i s) over the sets (\mathbb{S}_i s) of hydrophilic atoms over \mathbb{N} are on average 1.75-fold larger than those for the corresponding η_o s for hydrophobic atoms. In fact not only the hydrophilic atoms have larger surface areas the η_s^- s for the sets (\mathbb{S}^- s) of the surface atoms with negative partial charges are on average larger than the η_s^+ s (Fig. 2a and Table 2), this is consistent with the preference of water as a protic solvent for anions over cations. Moreover though both $A_o > A_i$ and $A^+ > A^-$ for either folded or unfolded structures, their ratios decrease upon folding (Table 2). Taken together it suggests that folding into a native state not only turns a protein into a capacitor but also maximizes its hydrogen bonding interaction with solvent with as little disruption to solvent structure as possible.

Though both average-partial charge and average-atomic area contribute to protein-solvent interaction their changes with protein size are somewhat complicated. For example, both of them decrease with protein size by power laws and their decreases are faster for small structures with $n < 2 \times 10^4$. In addition the distributions around their means are not symmetrical especially for average-atomic areas (Figs. 1a and 2a). The non-uniformity in their decreases with protein size implies that neither of them alone could properly describe protein-solvent interaction because its strength per exposed atom is expected to be statistically independent of size. In contrast to average-partial charge and average-atomic area, area-weighted surface charges (q_s^+ , q_s^- and q_s) change linearly with protein size (supplementary materials) and moreover area-weighted surface densities (σ_s^+ , σ_s^- and σ_s) are almost independent of size (Fig. 2b). In addition the distributions around their means are rather symmetrical as indicated by the very small differences between their means and medians even for small-sized structures in sets \mathbb{M}_f and \mathbb{M}_u (Table 3). Taken together it shows that SES properties that are functions of either charge or both surface area and charge provide a better description to protein-solvent interaction than area alone does. Previous applications [13, 9, 14, 10] have focused mainly on area alone (either ASA or SEA) and their usefulness for quantifying protein-solvent interaction remains to be controversial [37, 38, 39]. As shown here, our large-scale analyses of SEAs and SES-defined physical properties over both folded and unfolded structures demonstrate the importance of surface charge in protein-solvent interaction and also explains the inadequacy of using area alone for its evaluation. Furthermore, the statistical values for SES-defined properties and power laws obtained for the set of monomeric (\mathbb{M}) could be used to quantify the changes induced by ligand binding where the ligand is either DNA or small-molecule compound or another protein [21].

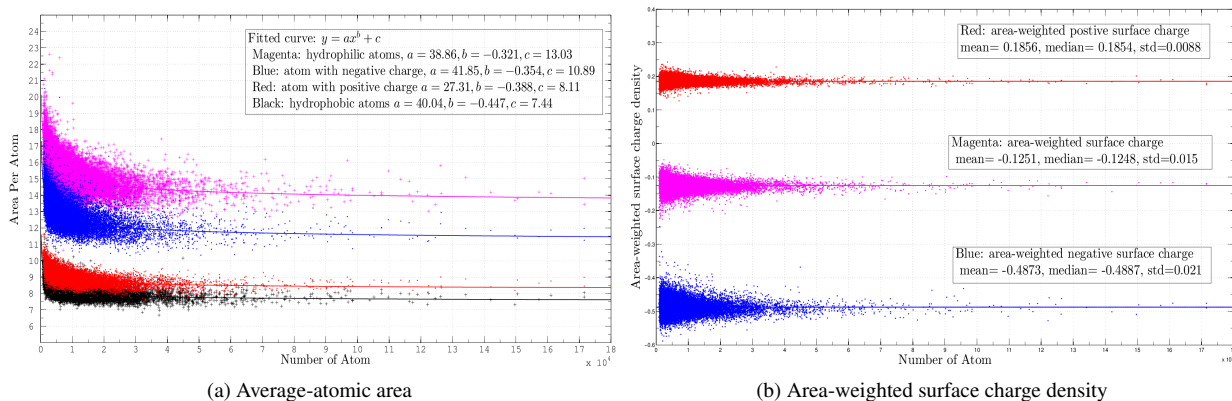


Figure 2: **Average-atomic areas and area-weighted surface charge densities.** (a) The average-atomic areas η_i , η_o and η_s^+ , η_s^- over \mathbb{N} . The fitted power laws, $y = ax^b + c$, shown in the insert all have negative b s and thus the values of parameters c could be used to compare their average-atomic areas. For example, the parameter c for η_s is 1.75-fold larger than that for η_o s. The y-axis is average-atomic area with a unit of \AA^2 per atom. (b) The area-weighted surface charge densities of σ_s^+ , σ_s^- and σ_s . The three lines indicate their respective means. The y-axis is area-weighted surface charge density in coulomb per atom. The x-axes in (a, b) are the total number of atoms in a protein.

Structures	σ_s^+	σ_s^-	σ_s	$\sigma_s^+ - \sigma_s^-$
\mathbb{M}_f	10.13, 10.11, 0.60	-22.42, -22.39, 1.46	-12.29, -12.23, 1.67	32.54, 32.55, 1.48
\mathbb{M}_u	10.50, 10.47, 0.43	-18.29, -18.24, 0.84	-7.79, -7.75, 0.92	28.80, 28.74, 0.96

Table 3: **The area-weighted surface charge and area-weighted surface dipole densities of the folded vs unfolded structures.** The three numbers in each cell are respectively mean, median and standard deviation with a unit of $10^{-2} \times$ coulomb. If we assume that the structures in \mathbb{M}_u are the representatives of unfolded states, then folding into a native state makes the surface slightly more positive but drastically more negative.

3.2 The geometry of SES

One advantage of SEA over ASA is that the former includes both convex and concave areas while the latter has only convex ones. Using SES we could define a geometrical property $r_{cc}(i) = \frac{a_p(i)}{a_s(i)}$ for each surface atom i to estimate its local flatness and $r_{cc} = \frac{\sum_i a_p(i)}{\sum_i a_s(i)}$, $i \in \mathbb{T}$ (Eq. 8) for a set of atoms \mathbb{T} to estimate the overall flatness of their total surface. The ratio r_{cc} is possibly related to the VDW interaction [39, 24] between surface atoms and solvent since we have $d_{ap}(i) = r_a(i) + r_p$ where $d_{ap}(i)$ is the inter-atom distance between protein atom i and a solvent atom, $r_a(i)$ the VDW radius for atom i and r_p probe radius. In addition the larger the ratio is, the more flat the surface, the smaller the surface tension and thus stronger the interaction with solvent. We also expect that the natural selection must have optimized protein-solvent interaction in terms of surface geometry via the maximization of the concave-convex ratio for hydrophobic atoms since VDW attraction is assumed to be the main factor for their solvation in polar solvent [24]. Indeed as shown in Fig. 3a the r_{cc} s for the sets of the hydrophobic atoms (A_o s) over \mathbb{N} are about 40% larger than those for the A_i s. Moreover r_{cc} s increase with protein size via well-fitted power laws (Fig. 3a) and the increase becomes more slowly when the number of atoms $n > 2.0 \times 10^4$. With more and more surface atoms it becomes increasingly possible to form flatter and flatter surface and consequently better and better protein-solvent interaction as far as surface geometry is concerned. Most interestingly, in stark contrast with the r_{cc} s over \mathbb{M}_f , the same r_{cc} s over \mathbb{M}_u are several-fold smaller and do not change with protein size (Fig. 3b). Taken together it shows that concave-convex ratio r_{cc} is a geometrical property relevant to protein-solvent interaction possibly via the VDW attraction between surface atoms and solvent.

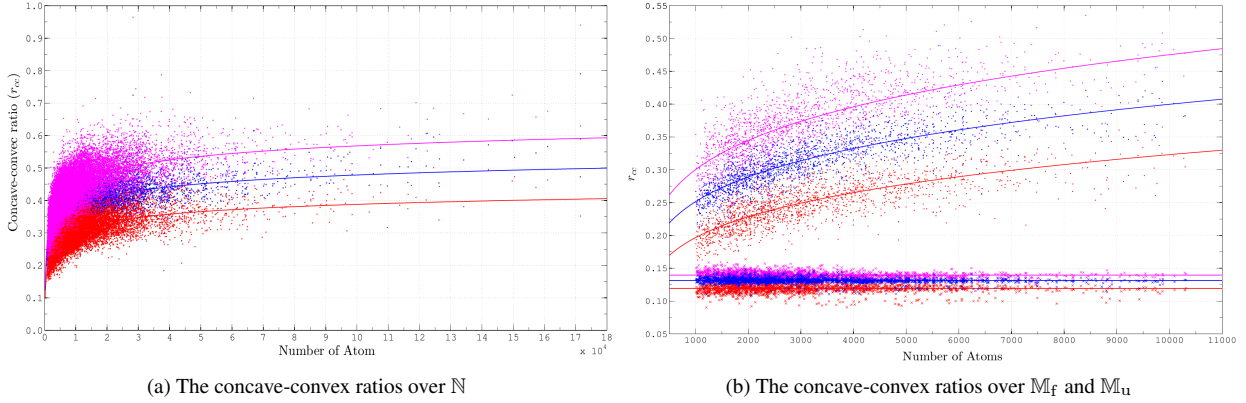


Figure 3: **Concave-convex ratio** r_{cc} . **(a)** The r_{cc} s for the hydrophilic (set \mathbb{S}_i and colored in red), hydrophobic (\mathbb{S}_o in blue) and all the atoms (in magenta) over \mathbb{N} . The three curves represent the fitted power laws $r_{cc}(n) = an^b + c$ shown in the insert. The b s are all negative so the parameter $c = \lim_{n \rightarrow \infty} r_{cc}(n)$ could be used to compare their concave-convex ratios. **(b)** The r_{cc} s of both folded and unfolded structures. The three curves are fitted power laws respectively for the sets of hydrophilic (colored in red), hydrophobic (in magenta) and all the atoms (in blue) over \mathbb{M}_f while the three lines indicate their means over \mathbb{M}_u .

3.3 Hydrophobicity scale

As described above the changes with protein size or upon unfolding of most SES-defined physical and geometrical properties follow well-fitted power laws. These properties are defined with the assignment of area and charge to individual atoms rather than individual residues. However the pertinent experimental data such as hydrophobicity scales are available only at residue-level. In this section we first describe the correlations between five known hydrophobicity scales [17, 18, 19, 20] and a dozen of physical and geometrical properties computed for each of 20 amino acid residues (Table 4) and then discuss their significance for protein-solvent interaction in general and folding in particular since hydrophobic effect is thought to be the driving force for the latter [22, 23]. We use Kyte-Doolittle scale as a reference since it incorporates both experimental data and computational surveys from several sources. The seven SES-defined electrical properties include net positive and negative surface charges, Q^+ and Q^- , area-weighted positive and negative surface charges, q^+ and q^- , as well as their differences $Q^+ - Q^-$ and $q^+ - q^-$ and the area-weighted surface charges (q_i s) of the hydrophilic atoms for a residue. The five geometrical properties include total SEA, the SEAs of hydrophilic, positive and negative-charged atoms as well as concave-convex ratio r_{cc} . Their correlations with the five scales are assessed by the goodness of fitting to either a linear equation or a power law. As shown in Table 4 the seven electrical properties in general fit to the five scales better than the five geometrical properties such as A and r_{cc} do. The best correlations exist between four SES-defined electric properties, Q^- , q^+ , $(q^+ - q^-)$ and $Q^+ - Q^-$, and the five scales. By comparison SEA (A) alone does not fit as well to the five scales. In fact except for r_{cc} the fitting between SEA and the five scales are the worst among the twelve properties. Previously the contribution of surface to protein-solvent interaction has been evaluated using mainly areas including both surface area and buried average area [40]. Furthermore it is assumed that there is a hydrophobic component ΔG_{hyd} of ΔG_{solv} that increases linearly with area A , and the assumption is widely used in implicit solvent models [39]. However the results presented here and in section 3.1 show that surface charge and electrical properties are more important than surface area in terms of their contributions to protein-solvent interaction. On the other hand, since strong correlations exist between either q^+ or $(q^+ - q^-)$ and the five scales we could interpret the fitted solvation parameters (σ_i s) [7, 8] in solvation free energy-surface area relation, $\Delta G_{\text{solv}} = \sum_i \sigma_i ASA_i$ as surface charges since ASA_i is to a good extent proportional to the SEA for the same residue.

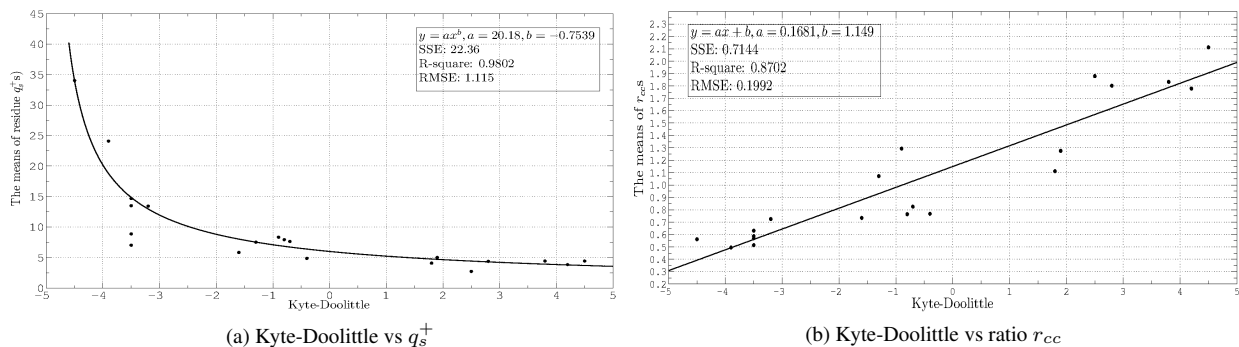


Figure 4: **The means of net positive surface charges and concave-convex ratios of 20 residues versus Kyte-Doolittle hydrophobicity scale.** (a) The means of net positive surface charges (q_s^+ s) of 20 residues versus Kyte-Doolittle scale. The curve is a best-fitted power law. The y-axis is the means of q_s^+ s for 20 residues in coulomb. (b) The means of concave-convex ratios (r_{cc} s) of 20 residues versus Kyte-Doolittle scale. The line is a best-fitted linear equation. The y-axis is the means of r_{cc} s for 20 residues. The x-axes in both (a, b) are Kyte-Doolittle scale.

3.4 The statistical distributions and power laws for SES-defined physical and geometrical properties

At present the details of protein-solvent interaction could only be obtained through all-atom MD simulation with either explicit or implicit solvent models. However MD with explicit solvent suffers from convergence problem while implicit models rely on a prior values for dielectric constants especially the dielectric constants near a protein surface or inside a protein [28]. For example accurate dielectric constant for protein surface is the key for the computation of solvation free energy [28] via electrostatic interaction. However the accurate determination of such dielectric constants remains to be a very challenging problem at present. As described above we have found a dozen of SES-defined electrical and geometrical properties that are likely to be important for protein-solvent interaction. Their statistical distributions and the power laws governing their changes with protein size or upon protein unfolding obtained on large sets of known structures should be useful for the quantification of solvation and hydrophobic effect using well-known theories on anion solutes in protic solvent [25, 26] or PLDL solvent model [27, 28]. In addition, the statistical values and power laws could be used to restraint the folding space of a protein and thus could serve as a term in an empirical scoring function for protein structure prediction [30] or a quantity for quality control in structure determination [31].

4 Conclusion

A robust and accurate algorithm for the computation of solvent excluded surface (SES) has been developed and applied to a large set of soluble proteins with crystal structures. We discover that all the soluble proteins have net negative surface charge and thus soluble proteins behave like a capacitor in solution. We have also identified a dozen of SES-defined physical and geometrical properties that are relevant to protein-solvent interaction based on their changes with protein size and upon protein unfolding as well as the strong correlation between them and five known hydrophobicity scales on a residue level. Most interestingly in contrast to previous emphasis on surface area we found that surface charge makes larger contribution to protein-solvent interaction than area does. These findings are consistent with water being a protic solvent that prefers anions over cations and show that folding into a native state is to optimize surface negative charge rather to minimize hydrophobic surface area. They suggest that the optimization of protein solvation through natural selection is achieved by (1) universal enrichment of surface negative charge, (2) increased surface areas for hydrophilic atoms for better hydrogen bonding with solvent, and (3) higher concave-convex ratio for hydrophobic atoms for better VDW attraction with solvent.

	Q^+	Q^-	A	A^+	A^-	A_i	q_s^+	q_s^-	q_i	p_r	p_s	r_{cc}
KD	0.92 ^b	0.96 ^b	0.94 ^b	0.93 ^b	0.94 ^b	0.89 ^b	0.98 ^b	0.90 ^b	0.85 ^b	0.94 ^b	0.96 ^b	0.87 ^a
EW	0.86 ^a	0.92 ^b	0.68 ^a	0.91 ^b	0.52 ^b	0.85 ^a	0.96 ^b	0.83 ^a	0.82 ^a	0.85 ^a	0.91 ^b	0.71 ^a
GES	0.83 ^a	0.89 ^a	0.71 ^a	0.90 ^b	0.52 ^a	0.88 ^a	0.85 ^a	0.93 ^a	0.82 ^a	0.89 ^a	0.89 ^a	0.51 ^a
JANIN	0.95 ^b	0.91 ^b	0.68 ^b	0.79 ^b	0.88 ^b	0.94 ^b	0.96 ^b	0.87 ^b	0.84 ^b	0.94 ^b	0.92 ^b	0.90 ^a
EXP	0.85 ^a	0.93 ^b	0.65 ^a	0.65 ^a	0.93 ^b	0.65 ^a	0.85 ^b	0.93 ^b	0.93 ^b	0.90 ^b	0.93 ^b	0.63 ^a
Average	0.88	0.92	0.73	0.84	0.76	0.84	0.92	0.89	0.85	0.90	0.92	0.72

Table 4: **The five hydrophobicity scales versus twelve SES-defined physical and geometrical properties.** The five scales are respectively Kyte-Doolittle (KD) [18], Eisenberg-Weiss(EW) [19], Goldman-Engelman-Steitz(GES) [20], Janin(JANIN) [17] and experimental hydrophobicity scales. The data for experimental scale is taken from Table xx of Kyte-Doolittle paper [18]. The twelve properties are computed over sets of atoms belonging to individual residues. Among them the seven properties, A , A^+ , A^- , A_i , q^+ , q^- , q_i and r_{cc} (Eqs. 2-8), are defined in section 2. The first two columns are respectively positive surface charge $Q^+ = \sum_i e(i)$, $e(i) > 0$ and negative surface charge $Q^- = \sum_i e(i)$, $e(i) < 0$. The 9th column q_i is the total area-weighted surface charge for all the exposed hydrophilic atoms of a residue. The 10th and 11th columns are respectively $p_r = Q^+ - Q^- = \sum_i e^+(i) - \sum_j e^-(j)$ and $p_s = q^+ - q^- = \sum_i a(i)e^+(i) - \sum_j a(j)e^-(j)$ where i is an exposed atom of a residue with positive partial charge and j an exposed atom with negative charge. For each residue we first compute the twelve properties over set \mathbb{M}_r and then compute their means. Finally the correlations between their means and the five scales are assessed by fitting them to either a linear equation $y = ax + b$ (indicated by superscript ^a) or a power law $y = ax^b$ (indicated by superscript ^b) where x is a hydrophobicity scale and y one of the twelve properties. The number in each cell is the coefficient of determination R_{square} . The last row is the average of R_{square} s.

References

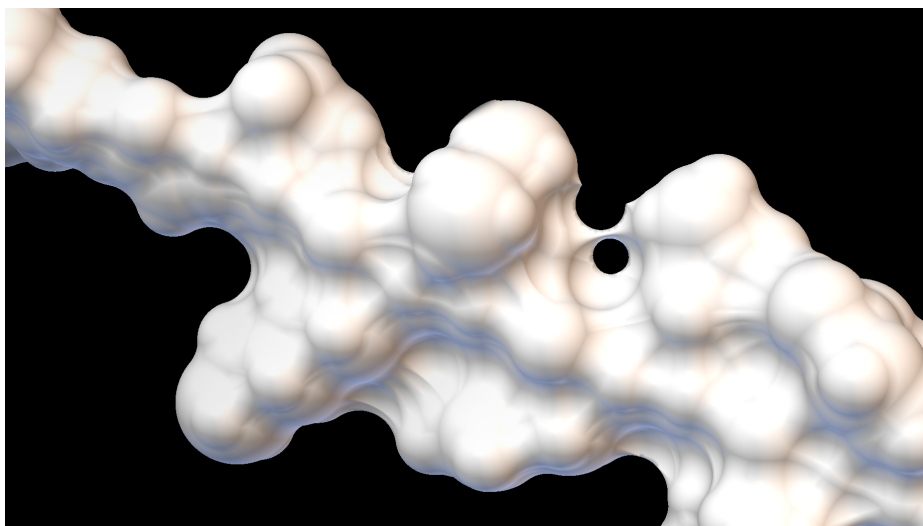
- [1] J. C. Kendrew, R. E. Dickerson, B. E. Strandberg, R. G. Hart, D. R. Davies, D. C. Phillips, and V. C. Shor. Structure of Myoglobin: A Three-Dimensional Fourier Synthesis at 2Å Resolution. *Nature*, 185:422–427, February 1960.
- [2] B. Lee and F. M. Richards. The interpretation of protein structures: Estimation of static accessibility. *Journal of Molecular Biology*, 55(3):379–400, 1971.
- [3] Robert B. Hermann. Theory of hydrophobic bonding. II. correlation of hydrocarbon solubility in water with solvent cavity surface area. *The Journal of Physical Chemistry*, 76(19):2754–2759, 1972.
- [4] F. M. Richards. Areas, volumes, packing, and protein structure. *Annual Review of Biophysics and Bioengineering*, 6(1):151–176, 1977. PMID: 326146.
- [5] C. Chothia. Hydrophobic bonding and accessible surface area in proteins. *Nature*, 248:338–339, 1974.
- [6] J. A. Reynolds, D. B. Gilbert, and C. Tanford. Empirical correlation between hydrophobic free energy and aqueous cavity surface area. *Proc. Natl. Acad. Sci. USA*, 71(8):2925–2927, 1974.
- [7] D. Eisenberg and A. D. Andrew D. McLachlan. Solvation energy in protein folding and binding. *Nature*, 319:199–203, 1986.
- [8] T. Ooi, M. Oobatake, G. Nmmethy, and H. A. Scheraga. Accessible surface areas as a measure of the thermodynamic parameters of hydration of peptides. *Proc. Natl. Acad. Sci. USA*, 84(10):3086–3090, 1987.
- [9] K. A. Sharp, A. Nicholls, R. F. Fine, and B. Honig. Reconciling the magnitude of the microscopic and macroscopic hydrophobic effects. *Science*, 252(5002):106–109, 1991.
- [10] B. R. Brooks, C. L. Brooks, A. D. Mackerell, L. Nilsson, R. J. Petrella, B. Roux, Y. Won, G. Archontis, C. Bartels, S. Boresch, A. Caflich, L. Caves, Q. Cui, A. R. Dinner, M. Feig, S. Fischer, J. Gao, M. Hodoseck, W. Im, K. Kuczera, T. Lazaridis, J. Ma, V. Ovchinnikov, E. Paci, R. W. Pastor, C. B. Post, J. Z. Pu, M. Schaefer, B. Tidor, R. M. Venable, H. L. Woodcock, X. Wu, W. Yang, D. M. York, and M. Karplus. Charmm: The biomolecular simulation program. *Journal of Computational Chemistry*, 30(10):1545–1614, 2009.
- [11] M. L. Connolly. The molecular surface package. *Journal of Molecular Graphics*, 11(2):139–141, 1993.
- [12] M. F. Sanner, A. J. Olson, and J. Spehner. Reduced surface: An efficient way to compute molecular surfaces. *Biopolymers*, 38(3):305–320, 1996.
- [13] C. Chothia. The nature of the accessible and buried surfaces in proteins. *Journal of Molecular Biology*, 105(1):1–12, 1976.
- [14] H. S. Ashbaugh, E. W. Kaler, and M. E. Paulaitis. A universal surface area correlation for molecular hydrophobic phenomena. *Journal of the American Chemical Society*, 121(39):9243–9244, 1999.

- [15] Y. Hemajit Singh, M. Michael Gromiha, Akinori Sarai, and Shandar Ahmad. Atom-wise statistics and prediction of solvent accessibility in proteins. *Biophysical Chemistry*, 124(2):145 – 154, 2006.
- [16] Lauren H. Kapcha and Peter J. Rossky. A simple atomic-level hydrophobicity scale reveals protein interfacial structure. *Journal of Molecular Biology*, 426(2):484–498, 2014.
- [17] J. Janin. Surface and Inside Volumes in Globular Proteins. *Nature*, 277:491–492, February 1979.
- [18] Jack Kyte and Russell F. Doolittle. A simple method for displaying the hydropathic character of a protein. *Journal of Molecular Biology*, 157(1):105–132, 1982.
- [19] D. Eisenberg, R. M. Weiss, and T. C. Terwilliger. The hydrophobic moment detects periodicity in protein hydrophobicity. *Proc. Natl. Acad. Sci. USA*, 81(1):140–144, 1984.
- [20] D. M. Engelman, T. A. Steitz, and Goldman. A. Identifying nonpolar transbilayer helices in amino acid sequences of membrane proteins. *Annual Review of Biophysics and Biophysical Chemistry*, 15(1):321–353, 1986. PMID: 3521657.
- [21] Lincong Wang. The contributions of surface charge and geometry to protein-ligand interaction. *Manuscript in preparation*.
- [22] W. Kauzmann. Thermodynamics of unfolding. *Nature*, 325:763–764, February 1987.
- [23] K. A. Dill. Dominant forces in protein folding. *Biochemistry*, 29(31):7133–7155, 1990. PMID: 2207096.
- [24] R. L. Baldwin. Dynamic hydration shell restores kauzmanns 1959 explanation of how the hydrophobic factor drives protein folding. *Proc. Natl. Acad. Sci. USA*, 111(36):13052–13056, 2014.
- [25] Lars Onsager. Electric moments of molecules in liquids. *Journal of the American Chemical Society*, 58(8):1486–1493, 1936.
- [26] C. Tanford and J. G. Kirkwood. Theory of protein titration curves. i. general equations for impenetrable spheres. *Journal of the American Chemical Society*, 79(20):5333–5339, 1957.
- [27] A. Warshel and M. Levitt. Theoretical studies of enzymic reactions: Dielectric, electrostatic and steric stabilization of the carbonium ion in the reaction of lysozyme. *Journal of Molecular Biology*, 103(2):227–249, 1976.
- [28] Arieh Warshel, Pankaz K. Sharma, Mitsunori Kato, and William W. Parson. Modeling electrostatic effects in proteins. *Biochimica et Biophysica Acta (BBA) - Proteins and Proteomics*, 1764(11):1647–1676, 2006.
- [29] Aleksandr V. Marenich, Christopher J. Cramer, and Donald G. Truhlar. Universal solvation model based on solute electron density and on a continuum model of the solvent defined by the bulk dielectric constant and atomic surface tensions. *The Journal of Physical Chemistry B*, 113(18):6378–6396, 2009. PMID: 19366259.
- [30] Pascal Benkert, Silvio C. E. Tosatto, and Dietmar Schomburg. Qmean: A comprehensive scoring function for model quality assessment. *Proteins: Structure, Function, and Bioinformatics*, 71(1):261–277, 2008.
- [31] Pradeep Kota, Feng Ding, Srinivas Ramachandran, and Nikolay V. Dokholyan. Gaia: automated quality assessment of protein structure models. *Bioinformatics*, 27(16):2209–2215, 2011.
- [32] A. T. Brunger. Version 1.2 of the Crystallography and NMR System. *Nature Protocol*, 2:2728–2733, February 2007.
- [33] J. Michael Word, Simon C. Lovell, Jane S. Richardson, and David C. Richardson. Asparagine and glutamine: using hydrogen atom contacts in the choice of side-chain amide orientation1. *Journal of Molecular Biology*, 285(4):1735–1747, 1999.
- [34] M. F. Perutz. Electrostatic effects in proteins. *Science*, 201(4362):1187–1191, 1978.
- [35] D. L. Mobley, A. E. Barber II, C. J. Fennell, , and K. A. Dill. Charge asymmetries in hydration of polar solutes. *The Journal of Physical Chemistry B*, 112(8):2405–2414, 2008. PMID: 18251538.
- [36] T. Simonson and D. Perahia. Internal and interfacial dielectric properties of cytochrome c from molecular dynamics in aqueous solution. *Proc. Natl. Acad. Sci. USA*, 92(4):1082–1086, 1995.
- [37] C. Tanford. Interfacial free energy and the hydrophobic effect. *Proc. Natl. Acad. Sci. USA*, 76(9):4175–4176, 1979.
- [38] X. Pang and H. X. Zhou. Poisson-Boltzmann calculations: van der Waals or molecular surface? *Commun Comput Phys*, 13(1):1–12, 2013.
- [39] R. C. Harris, B., and B. M. Pettitt. Effects of geometry and chemistry on hydrophobic solvation. *Proc. Natl. Acad. Sci. USA*, 111(41):14681–14686, 2014.
- [40] G. D. Rose, A. R. Geselowitz, G. J. Lesser, R. H. Lee, and M. H. Zehfus. Hydrophobicity of amino acid residues in globular proteins. *Science*, 229(4716):834–838, 1985.

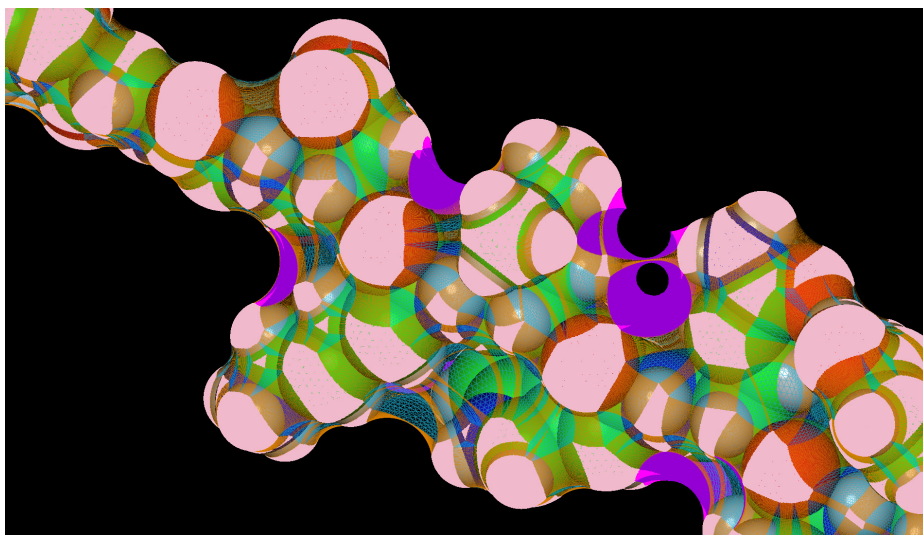
Supplementary Information

S1: The comparison of the surfaces by MSMS, PyMOL and our SES program

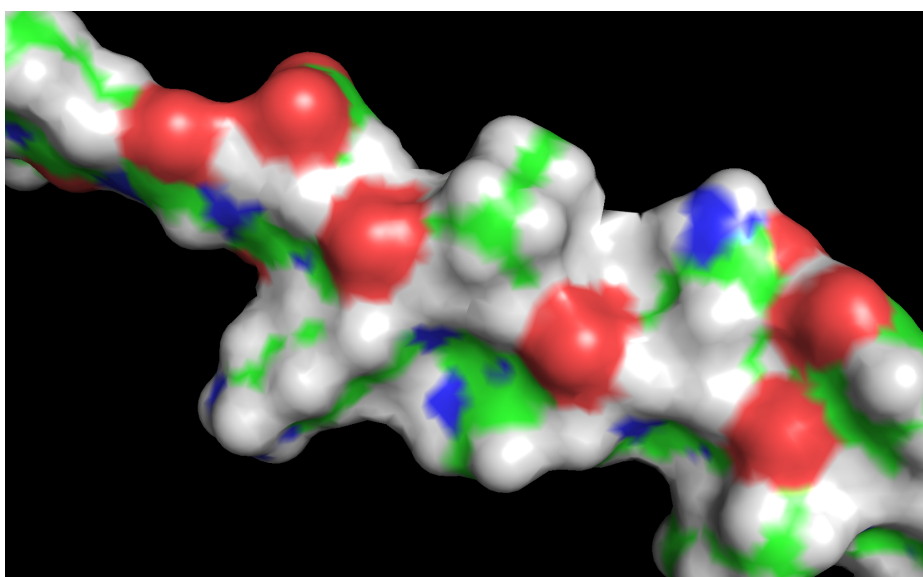
The structure used for the comparison is a peptide (min1.pdb) downloaded from an Amber tutorials website (<http://ambermd.org/tutor>). The MSMS SES surface is generated by setting a probe radius=1.2Å, density=100.0 and high density=200.0. During the surface computation the atomic radii for the following three atoms, 66, 69 and 97, are increased by 0.1Å. As indicated by the four arrows in Fig. S1a the regions where the PAA areas interact with each other are relatively rough. In the contrast the four corresponding regions (colored in violet) in our SES surface (Fig. S1b) are as smooth as the rest. As a reference the surface (Fig. S1c) generated by a popular molecular visualization program PyMOL lacks the details especially for the four intersecting PAA regions.



(a) MSMS



(b) Our SES Program



(c) PyMOL

Figure S1: The surfaces by MSMS, our program and PyMOL.